Model Predictive Control for Slurry Pipeline Transportation of a Cutter Suction Dredger

Changyun Wei[a,b], Yi Wei[a,b] and Ze Ji[c,*]

[a]*College of Mechanical and Electrical Engineering, Hohai University, China*
[b]*Engineering Research Center of Dredging Technology of Ministry of Education, Hohai University, China*
[c]*School of Engineering, Cardiff University, Cardiff CF24 3AA, United Kingdom*

ARTICLE INFO

Keywords:
Pipeline Transportation
Model Predictive Control
Slurry Pumps
Automated Control
Cutter Suction Dredgers

ABSTRACT

Cutter Suction Dredgers (CSDs) are a special type of ships designed for construction and maintenance projects of ocean and offshore engineering. During the dredging operation, CSDs can excavate nearly all kinds of soil on the sea bed, and then the dredged materials with coarse particles need to be sucked up by a slurry pump and transported to a disposal area through a long-distance pipeline. In order to avoid sedimentation of slurry in pipeline transportation, the flow rate must be maintained within a reasonable range. Otherwise, the pipeline can be blocked when the slurry density is too high. In this paper, we present a Model Predictive Control (MPC) approach to manipulate the flow rate of slurry in pipeline transportation for a CSD. To demonstrate the advantages of our proposed approach, we also implement three Proportional-Integral-Derivative (PID) controllers (i.e., conventional PID, Fuzzy-PID, and LQR-PID) to make a direct comparison. Moreover, in order to evaluate the effectiveness of our proposed approach in real scenarios, we have, in particular, built a slurry pipeline transportation platform. Both the simulation and experimental results show that our proposed MPC approach is more effective than other PID controllers in controlling the flow rate in the slurry pipeline transportation problem. The proposed approach can provide a guideline for the automated control of the slurry pump for a CSD.

1. Introduction

CSDs are a special type of ships for construction and maintenance projects of ocean and offshore engineering, such as harbour deepening and land reclamation (Wang et al., 2020). Comparing with other dredging vessels, CSDs can excavate nearly all kinds of soil (i.e., sand, clay or rock) on the sea bed by a cutter head (Tang et al., 2009). Then, the dredged materials need to be sucked up by a dredger pump and transported to a disposal area through a long-distance pipeline, as shown in Fig. 1. During the dredging process of a CSD, the pipeline transportation system consumes most energy, and, in addition, control of the flow rate of the slurry is essential for its safe operation. Therefore, the automated control of the slurry pump will be beneficial to both the operators and dredging companies.

In comparison with other slurry transportation in pipelines, the control of dredged materials faces the following challenges. Firstly, the CSD is usually located several kilometres away from the final disposal area, and the dredged slurry must be transported to the area with a high concentration (Bai et al., 2019). Secondly, the dredged slurry differs from a homogeneous material, such as mineral slurry (Sinha et al., 2017), oil (Priyanka et al., 2018) and coal fly ash (Singh et al., 2017), and may include coarse particles of hard rocks that vary in size (Ting et al., 2019). Moreover, the distribution of solid particles along the pipeline is uneven, and the

particles tend to accumulate at the bottom of the pipeline because of gravity. Thus, if the flow rate is too slow, the solid particles of slurry will be deposited on the bottom of the pipeline, causing blockage accidents (Wei et al., 2019); however, if the flow rate is too high, the solid particles will wear down the pipeline and lead to a rupture. In order to resolve the above problems, the flow rate must be maintained within an acceptable range in the pipeline. To this end, this work aims at providing a Model Predictive Control (MPC) approach to manipulating the flow rate of slurry for a CSD.
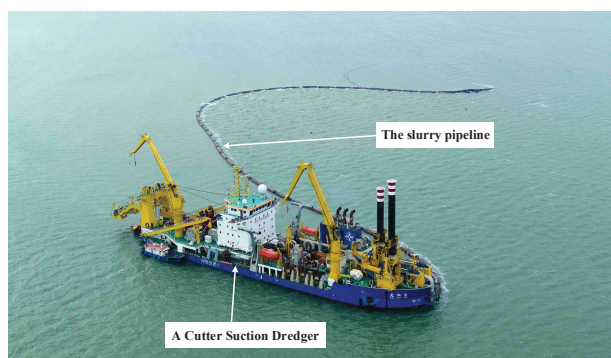
Figure 1: The cutter suction dredger with the slurry pipeline transportation system.

Many methods have been studied to address the flow control problem in pipeline transportation. For example, a Fuzzy-PID controller is designed to automatically regulate the flow rate of oil pipelines by controlling the pressure at distinct points (Priyanka et al., 2018). The flow rate control has also been achieved by managing the percentage of opening of the

control valves in oil pipelines by a PID controller (Priyanka et al., 2016). Similarly, a PID controller is utilized to control the flow rate of heavy oil in pipelines by controlling the vibration on a motor (Razvarz et al., 2019), but the effectiveness of the PID controller is only proved by numerical simulations. So far many existing methods of controlling the flow rate in pipelines focus on transporting homogeneous materials, but little research has studied the automated control approach to transporting the slurry with coarse particles in pipelines. In this work, we focus on the slurry pipeline transportation system of a CSD, and we also implement three PID controllers as the baseline, i.e., a conventional PID controller, a Fuzzy-PID controller and a Linear Quadratic PID controller.

Process control in industry often involves time delays. It is difficult for a simple feedback controller to handle the process control problem with time delays (Bobal et al., 2013). Slurry pipeline transportation is a kind of control systems with large inertia, large time delays and time variation. To realize steady control of the flow rate of slurry, the controller must have the adaptive ability of responding to the dynamic changes of the external environment. When the relative time delay is very large, the predictive control can provide a possible solution to such a problem (Grüne and Pannek, 2017). Among the feasible solutions, the MPC (Vazquez et al., 2016; Wang et al., 2015) has been successfully applied for controlling the processes with time delays. MPC is a promising alternative because it can be easily used in multivariable systems and can predict the dynamic behaviour of the system. Moreover, nested control loops can be incorporated in a single loop, which is conductive to the implementation of such a control system (Morari and Lee, 1999; Kouvaritakis and Cannon, 2016). In this work, we will also look at a MPC approach to the slurry pipeline transportation of a CSD.

With regard to the performance of MPC methods, a simulation study has evaluated two MPC methods (i.e., dynamic matrix control and generalized predictive control) in comparison with a classical PID controller (Ramdani and Grouni, 2017), and the simulation results can show the advantages of the two MPC methods. Similarly, a linear MPC and the predictive function control are also compared with the PI regulator (Rullo et al., 2014). Another recent work has presented a MPC method to address the cell generation system, in comparison with a PID controller (Long et al., 2015). We can identify that many studies have shown the effectiveness of MPC methods by comparing with PID controllers, but the performance is only evaluated in simulation environments in most cases. In this work, the proposed MPC approach will also be evaluated in comparison with three PID controllers, and, in addition, the experiments are carried out both in simulations and on a physical platform.

In this paper, we aim at introducing a MPC approach to the slurry pipeline transportation system of a CSD. The main contributions of this work can be summarized as follows:

1. To our best knowledge, we are the first to present a MPC approach to address the slurry pipeline transportation system of a cuter suction dredger.

2. In order to validate the advantages of the proposed MPC approach, its performance is compared with other three PID controllers, i.e., a conventional PID controller, a Fuzzy-PID controller and a Linear Quadratic PID controller.

3. In order to prove the feasibility of stabilizing the flow control of slurry in real environments, we have, in particular, designed a slurry pipeline transportation platform. We carry out extensive experiments both in simulations and on the physical platform to validate the robustness of the proposed approach.

The paper is organized as follows. We describe the model of the slurry pipeline transportation system and present the proposed MPC approach in Section 2. In order to evaluate the proposed MPC approach, we also design three PID controllers as the baseline in Section 3. Then, we introduce the designed experiment platform and discuss the results in Section 4. Finally, a brief conclusion is drawn to summarize the study in Section 5.

2. Model Predictive Control Approach

In this section, we first present the model of the slurry pipeline transportation system and then introduce the MPC approach studied in this work. We will detail how the proposed approach deals with the predictive model, rolling optimization and feedback regulation.

2.1. Slurry Pipeline Transportation System

As mentioned before, a CSD uses its cutter head to excavate hard rock or soil on the sea bed, and then the dredged materials will be sucked up by a slurry pump. The energy that can transport the sand-water mixture to the disposal area is provided by the slurry pump. The process of slurry pipeline transportation is illustrated in Fig. 2. In a CSD, the slurry

Figure 2: The process of the slurry pipeline transportation.

pump is driven by a motor, thus the flow rate can be adjusted by changing the rotation speed of the motor. To this end, the control variable is amplified by the analog signal output module to obtain the input value of the frequency converter, which can provide the input voltage to drive the motor. Afterwards, the input voltage can determine the rotation speed of the motor that directly drives the slurry pump units to transport the sand-water mixture. Finally, the desired flow rate in the pipeline can be obtained by adjusting the rotation speed of the pump.

Due to the presence of time delays in the slurry transportation problem, we choose a time-delay system. Based on the typical transfer function methodology, a local process model is established for the flow rate control in pipelines,

$$Gp_1(s) = \frac{k}{(Ts+1)^{na}} e^{-\tau s}, \tag{1}$$

where k denotes the open-loop gain of the system, T is the time constant of the inertia part of the system, na represents the order, and τ indicates the time delay. We do not separately model the correlations between the elements such as the transmission medium, the transmission distance, and transmission level of particulate matter. Instead, the system model is considered as a whole, and we can adopt differential evolution to identify the model parameters, which will be detailed in Section 4.1.1. Finally, the system model is represented by a second-order time-delay system,

$$Gp_1(s) = \frac{k}{(Tp_1 \cdot s + 1)(Tp_2 \cdot s + 1)} e^{-\tau s}, \qquad (2)$$

where k denotes the open-loop gain of the system, Tp_1 and Tp_2 are the time constants of the inertia part of the system. In order to verify the effectiveness and accuracy of the identified system model, experiments have been carried out to show that the system model can accurately describe the dynamics of he slurry transportation process.

2.2. Control Framework

The objective of our MPC approach is to obtain a sequence of control variables to optimize the future behaviour, taking account of the time delays and large inertia in slurry pipeline transportation. Such an automated control paradigm is realized based on the error between the reference trajectory and the predicted output. Thus, a model that can provide an accurate prediction of the future is essential for describing the dynamics of the system in predictive control. In this work, the proposed MPC approach to the slurry pipeline transportation is based on the model framework of the Dynamic Matrix Control (DMC) (Cutler and Ramaker, 1980), which uses step response of the system to make predictions. The general idea of the control framework is depicted in Fig. 3, where multi-step prediction is adopted to address the problem of the delay process. As shown in Fig. 3, the most
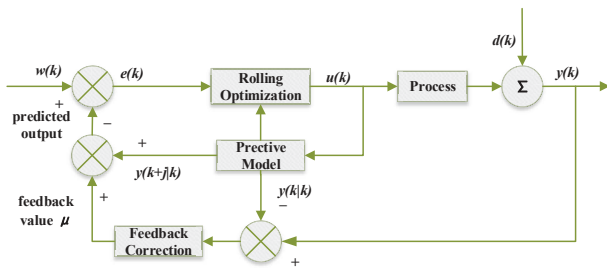
Figure 3: The control framework of the MPC approach.

important components of the MPC is the predictive model, rolling optimization, and feedback regulation. In the illustration, $y(k|k)$ denotes the current output by the predictive model at time k, $w(k)$ represents the reference trajectory, $e(k)$ means the error between the reference trajectory and predicted output, and $d(k)$ indicates the external disturbance.

The working mechanism of the MPC framework is described in Fig. 4. At time k, a finite-time open-loop problem is solved online based on the current state information, and

the first element of the control sequence (see Eq. (15)) is applied to the system. At time $k + 1$, the system will repeat the process of time k; the optimized problem will be refreshed with the next state. Compared to traditional methods, the optimal sequence is obtained by solving the open-loop problem online in MPC, but the feedback regulation mechanism enables the MPC to be a closed-loop system.
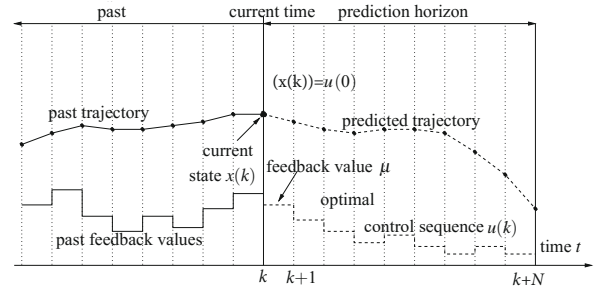
Figure 4: The working mechanism of the MPC at time t_n.

2.3. The Predictive Model

As one of the key component of the MPC framework, the predictive model consists of the step response coefficients $(a_1, a_2, \cdots a_p)$, in which a_i is the amplitude of the step response at the i-th sample step (Moon and Lee, 2009). The values of the step response at time k are used to describe the dynamics of the system. The step response curve of the identified system model Eq.(2) is shown in Fig. 5, where the value of a_p is close enough to the steady state.
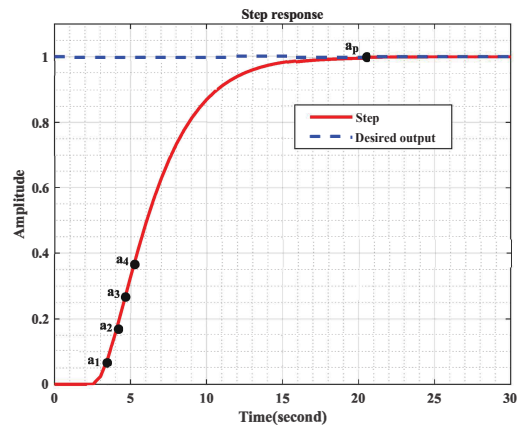
Figure 5: The step response curve of the slurry pipeline transportation system.

According to the properties of proportion and superposition of a linear system, the input $u(k-i)$ at time $k-i$ $(k \geq i)$ will contribute to the output $y(k)$ as

$$y(k) = \left\{ \begin{array}{ll} a_i \Delta u(k-i) & (1 \leq i < p) \\ a_p \Delta u(k-i) & (i \geq p) \end{array} \right\} \quad (i = 1, 2, \cdots, n). \qquad (3)$$

If the inputs at all the time step $k - i$ $(i = 1, 2 \cdots k)$ can be applied, according to the superposition of a linear system,

the output can be written as

$$y(k) = \sum_{i=1}^{p-1} [a_i \Delta u(k-i) + a_p \Delta u(k-i)]$$
$$+ \hat{\eta}(k+j/k) \quad (j = 1, 2, \cdots, n), \quad (4)$$

where $\hat{\eta}(k+j/k)$ is the predicted disturbance at time $t+j$. Based on the above equation, it is easy to obtain n ($n < p$) step prediction

$$\hat{y}(k+j/k) = \sum_{i=1}^{p-1} [a_i \Delta u(k+j-i) + a_p \Delta u(k+j-p)]$$
$$+ \hat{\eta}(k+j/k) \quad (j = 1, 2, \cdots, n). \quad (5)$$

Since we can only know the inputs before time k, we have to separate the contributions to the future output when utilizing the dynamic model. Then the above equation can be written as

$$\hat{y}(k+j/k) = \sum_{i=1}^{j} a_i \Delta u(k+j-i) + \sum_{i=j+1}^{p-1} [a_i \Delta u(k+j-i)$$
$$+ a_p \Delta u(k+j-p)] + \hat{\eta}(k+j/k) \quad (j = 1, 2, \cdots, n), \quad (6)$$

where the middle two terms represent the contributions of the past inputs to the system output, and we can have the n step prediction

$$y_0(k+j) = \sum_{i=j+1}^{p-1} [a_i \Delta u(k+j-i) + a_p \Delta u(k+j-p)].$$
$$(j = 1, 2, \cdots, n). \quad (7)$$

Eq. (6) can be written in matrix form as

$$\begin{pmatrix} \hat{y}(k+1) \\ \hat{y}(k+2) \\ \vdots \\ \hat{y}(k+n) \end{pmatrix} = \begin{pmatrix} a_1 & & & 0 \\ a_2 & a_1 & & \\ \vdots & \vdots & \ddots & \\ a_n & a_{n-1} & \cdots & a_1 \end{pmatrix}$$
$$\begin{pmatrix} \Delta u(k) \\ \Delta u(k+1) \\ \vdots \\ \Delta u(k+n-1) \end{pmatrix} + \begin{pmatrix} y_0(k+1) \\ y_0(k+2) \\ \vdots \\ y_0(k+n) \end{pmatrix}. \quad (8)$$

To increase the dynamic stability of the control system and the realizability of the control inputs, we decrease the vector of Δu from n to m dimensions

$$\begin{pmatrix} \hat{y}(k+1) \\ \hat{y}(k+2) \\ \vdots \\ \hat{y}(k+n) \end{pmatrix} = \begin{pmatrix} a_1 & & & 0 \\ a_2 & a_1 & & \\ \vdots & \vdots & \ddots & \\ a_n & a_{n-1} & \cdots & a_{n-m+1} \end{pmatrix}$$
$$\begin{pmatrix} \Delta u(k) \\ \Delta u(k+1) \\ \vdots \\ \Delta u(k+m-1) \end{pmatrix} + \begin{pmatrix} y_0(k+1) \\ y_0(k+2) \\ \vdots \\ y_0(k+n) \end{pmatrix}. \quad (9)$$

Eq. (9) can also be expressed by

$$\hat{Y} = A\Delta U + Y_0, \quad (10)$$

where $\hat{Y} = [\hat{y}(k+1), \hat{y}(k+2), \cdots, \hat{y}(k+n)]^T$ is a $n \times 1$ vector denoting the predicted trajectory of future output, $\Delta U = [\Delta u(k), \Delta u(k+1), \cdots, \Delta u(k+m-1)]^T$, ΔU is a $m \times 1$ vector of the input adjustment, $Y_0 = [y_0(k+1), \cdots, y_0(k+n)]^T$ denotes the vector of the unforced output trajectory, implying an open-loop prediction with Δu maintains constant, and $A \in \mathbb{R}^{n \times m}$ represents the dynamic matrix. The matrix A is a dynamic matrix that can reflect the dynamics of the control object, and it is entirely determined by the step response of the system. Here n and m indicate the prediction horizon and the control horizon respectively.

2.4. Rolling Optimization

In order to ensure that the system output can be as close as possible to the reference trajectory of the future output, the system need to select and apply the input adjustment vector ΔU at time k. As the predictive model of the system is based on dynamic response coefficients, we can minimize $J(k)$ to find an input adjustment vector,

$$J(k) = \sum_{i=1}^{n} Q[y(k+j) - w(k+j)]^2 + \sum_{j=1}^{m} R[\Delta u(k+j-1)]^2$$
$$= \|y(k+j) - w(k+j)\|_Q^2 + \|\Delta u(k+j-1)\|_R^2, \quad (11)$$

where $w(k+j) = \alpha^j y(k) + (1 - \alpha^j) y_r$ ($j = 1, 2, \cdots, n$), α ($0 < \alpha < 1$) is the softening factor, and $y(r)$ is the desired output. Then, the above equation can be abbreviated as

$$J(k) = \|Y - W\|_Q^2 + \|\Delta U\|_R^2. \quad (12)$$

Here $Q \in \mathbb{R}^{n \times n}$ and $R \in \mathbb{R}^{m \times m}$ denote the positive definite and weighted matrices. $Y = [y(k+1), \cdots, y(k+n)]^T$ is the system output, while $W = [w(k+1), \cdots, w(k+n)]^T$ denotes the reference trajectory of the future output, which is followed by the closed-loop responses to improve the robustness of the system. Then we can replace Y with the optimal predicted value of $\hat{Y}$ in Eq.(10), $J(K)$ can be written as

$$min \quad J = (A\Delta U + \hat{Y})^T Q (A\Delta U + \hat{Y}) + \Delta U^T R \Delta U. \quad (13)$$

The input adjustment vector ΔU is obtained by the derivation of Eq.(14),

$$\Delta U = (A^T Q A + R)^{-1} A^T Q (W - Y_0). \quad (14)$$

The above equation gives the optimal control sequence at time k, which is based purely on the predictive model. Because the presence of the model errors, weak nonlinear and other effects, the optimal control sequence cannot closely track the reference trajectory. It is impossible for the system to wait m time steps and then repeat Eq. (14); otherwise the system will inevitably cause large deviations and cannot suppress disturbances. Therefore, the first element of $\Delta u(k)$ is applied to the system, and the input adjustment vector can be obtained as shown in Eq.(15). Afterwards, the system applies $u(k)$ to the process model (see Eq. (2)).

$$\Delta u(k) = d^T (W - Y_0),$$
$$u(k) = u(k-1) + \Delta u(k), \quad (15)$$

where $d^T = C^T(A^TQA + R)^{-1}A^TQ$ and $C^T = [1, 0, \cdots, 0]$. Since A, Q are known and d can be identified offline, the online calculation of Δu is obtained from two vectors. The control strategy is to make new predictions, regulations, and optimizations by gathering the output data at time $k + 1$, when input adjustment vector $u(k)$ is applied to the system.

Rolling optimization does not mean that an offline calculation is enough to complete the entire optimization process. Instead, the optimization objective will change along with the control time, and the optimization process needs to be repeated accordingly. In other words, a local optimum is obtained and applied to the system at each time step, rather than trying to find a constant global optimum.

2.5. Feedback Regulation

Due to the dynamics of the external environment, there must be error between the predicted output and the system output. Since the system is only applied the first term of the optimal control sequence ΔU at time k, and the prediction of the future time steps can be represented as

$$\hat{Y}_p = a\Delta u(k) + Y_{p0}, \tag{16}$$

where $\hat{Y}_p = [\hat{y}(k+1/k), \hat{y}(k+2/k), \cdots, \hat{y}(k+p/k)]^T$ denotes p predicted outputs with the contribution of input adjustment vector Δu at time k. Similarly, $Y_{p0} = [y_0(k+1/k), y_0(k+2/k), \cdots, y_0(k+p/k)]^T$ represents p predicted outputs without the contribution of input adjustment vector Δu at time k. And $a = [a_1, a_2, \cdots a_p]^T$ is a vector denoting coefficients of the step response at the sample step.

Due to the uncertainty of the control objective, when the input adjustment vector Δu is applied into the system at time k, there is the feedback value μ between the system output $y(k+1/k)$ and the predicted output $\hat{y}(k+1/k)$ at time $k+1$,

$$\begin{aligned}\mu(k+1/k) &= y(k+1/k) - \hat{y}(k+1/k), \\ \hat{y}(k+1/k) &= y_0(k+1/k) + a_1\Delta u(k).\end{aligned} \tag{17}$$

Then we can weight the error and then regulate the predicted output for next prediction horizon as

$$\tilde{Y}_p = \hat{Y}_p + h\mu(k+1/k), \tag{18}$$

where $h = [h_1, h_2, \cdots, h_p]^T$ represents the adjustment vector, in general $h_1 = 1$. Moreover, $\tilde{Y}_p = [\tilde{y}(k+1/k), \tilde{y}(k+2/k), \cdots, \tilde{y}(k+p/k)]^T$ denotes the predicted output regulated by the feedback value at time k. The regulated $\tilde{Y}_p$ (except for the first item) is used as the unforced output trajectory for $t = k+2, ..., t = k+p+1$ times. We express the above relationship by

$$y_0(k+i/k+1) = \tilde{y}(k+i+1/k+1) \quad (i = 1, 2, \cdots, p-1), \tag{19}$$

And the last element in $Y_0(k+1)$ can be approximated by $\tilde{y}(k+p/k+1)$ at time $k+1$. Therefore, Eq. (19) can be further expressed as

$$Y_0(k+1) = S \cdot \tilde{Y}_p(k+1), \tag{20}$$

where S is defined as the shift matrix

$$S = \begin{bmatrix} 0 & 1 & 0 & \cdots & 0 \\ 0 & 0 & 1 & & \\ \vdots & \vdots & \vdots & \ddots & \\ 0 & 0 & 0 & \cdots & 1 \\ 0 & 0 & 0 & \cdots & 1 \end{bmatrix}.$$

The regulated predicted output ensures that the system can become a closed-loop feedback control problem to improve performance.

To summarize the MPC approach, it is mainly composed of the predictive model, the controller, and the regulator. The predictive model is responsible for providing the future predictions, while the controller determines the system dynamics. The regulator will play a role and come into operation only in the presence of prediction errors.

3. Design of PID Controllers for Comparison

In this section, we will briefly discuss the design of three PID controllers, i.e., a conventional PID controller, a Fuzzy-PID controller and a Linear Quadratic PID controller. The above controllers are considered as the baseline, which will be evaluated in comparison with our proposed MPC approach in the experiments in the next section.

3.1. Conventional PID Controller

Conventional Proportional-Integral-Derivative (PID) controllers have been extensively applied in many industrial automation and process control. It is widely used because of its versatility, high reliability, ease of operation, and effectiveness for most linear systems. A standard form of a PID controller has the expression of

$$u(t) = K_p e(t) + K_i \int e(t)dt + K_d \frac{de(t)}{dt}, \tag{21}$$

where $e(t)$ denotes the tracking error between the reference $w(t)$ and the system output $y(t)$, $d(t)$ indicates the external disturbance and K_p, K_i, K_d are the proportional, integral, and derivative gains, respectively. Fig. 6 illustrates how to implement a conventional PID controller. In this work, such
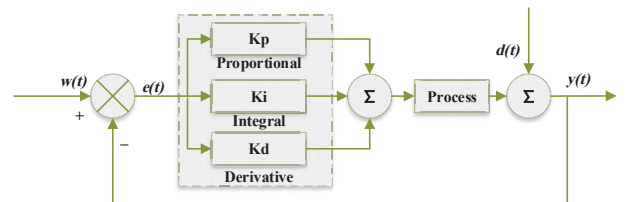
Figure 6: Illustration of the conventional PID controller.

a conventional PID controller is implemented and will be evaluated both in simulations and the physical platform.

3.2. Fuzzy-PID Controller

It is known to be difficult for conventional PID controllers to be applied in nonlinear and time-delay systems. As a

modified version, the Fuzzy-PID controller employs fuzzy logic but still remains the advantages of the conventional PID controllers. Although the structure is linear, but the PID gains are nonlinear functions of the input signals. The fuzzy control of the process model adopts linguistic variables instead of values, and the control gains are tuned manually, which generally cannot achieve the best possible performance. Fig. 7 depicts the structure of the Fuzzy-PID controller.
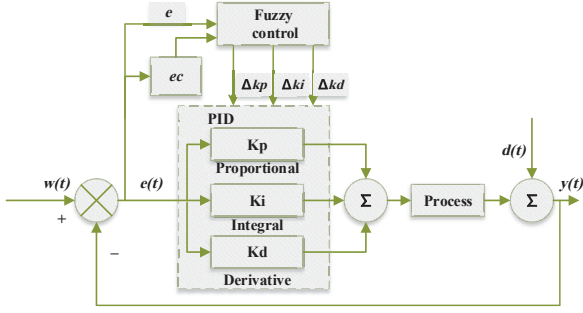
Figure 7: Illustration of the Fuzzy-PID Controller.

Similar to the conventional PID controller, $w(t)$ denotes the reference trajectory, and $e(t)$ indicates the tracking error signal between the reference trajectory and the system output $y(t)$. As shown in Fig. 7, the Fuzzy-PID controller takes the error e and the error rate ec as inputs and takes the increment of control gains (i.e., Δk_p, Δk_i, Δk_d) as the outputs. The above Fuzzy-PID control mechanism can be expressed by

$$\begin{cases} K_p = K_p' + \Delta k_p \\ K_i = K_i' + \Delta k_i \\ K_d = K_d' + \Delta k_d \end{cases}, \tag{22}$$

where K_p', K_i', K_d' are the constant control gains, and K_p, K_i, K_d are the modified control gains.

3.2.1. The Domain and Fuzzy Rules

In general, the range of system inputs and outputs of a fuzzy controller is referred to as the domain. In order to transform the input variables from the domain to the corresponding fuzzy sets, we present the quantization factor k_e, k_{ec} in the process of fuzzification. With different combinations of the error e and the error rate ec, the Fuzzy-PID controller is able to meet the self-adjustment requirements at different time steps, according to fuzzy rules, and to carry out online optimization of control gains K_p, K_i, and K_d. The design of fuzzy rules is generally based on the expert knowledge and a large number of experimental data.

In this work, the fuzzy rule settings between system inputs and outputs are shown in Table 1, with the linguistic labels: PB (Positive Big), PM (Positive Medium), PS (Positive Small), ZO (Zero), NS (Negative Small), NM (Negative Medium), and NB (Negative Big). The domain of the error e and the error rate ec are chosen as $[-8, +8]$, $[-8, +8]$, and the domain of the increment control gains Δk_p, Δk_i,

Table 1
The fuzzy rules used in the Fuzzy-PID controller.

	Δ kp	ec						
		NB	NM	NS	ZO	PS	PM	PB
	NB	PB	PB	PB	PB	PS	ZO	NS
	NM	PB	PB	PM	PM	ZO	NS	NM
	NS	PB	PM	PM	PS	NS	NM	NB
e	ZO	ZO	ZO	ZO	ZO	ZO	ZO	ZO
	PS	NB	NM	NS	PS	PM	PM	PB
	PM	NM	NS	ZO	PM	PB	PB	PB
	PB	NS	ZO	PS	PB	PB	PB	PB
	Δ ki	ec						
		NB	NM	NS	ZO	PS	PM	PB
	NB	NB	NB	NB	NB	PS	PS	PB
	NM	NB	NM	NM	NM	PM	PB	PB
	NS	NM	NS	NS	NS	PB	PB	PB
e	ZO	ZO	ZO	ZO	ZO	ZO	ZO	ZO
	PS	PB	PB	PB	NS	NS	NM	NB
	PM	PM	PB	PM	NM	NM	NB	NB
	PB	PB	PM	PS	NB	NB	NB	NB
	Δ kd	ec						
		NB	NM	NS	ZO	PS	PM	PB
	NB	PS	PS	ZO	ZO	ZO	PS	PS
	NM	NB	NB	NM	NS	NS	NM	NM
	NS	NB	NB	NM	NM	NS	NM	NM
e	ZO	ZO	ZO	ZO	ZO	ZO	ZO	ZO
	PS	NB	NB	NM	NS	NM	NM	NM
	PM	NB	NB	NM	NM	NM	NS	NB
	PB	PS	PS	ZO	ZO	ZO	PS	NB

and Δk_d are chosen as $[-0.05, +0.05]$, $[-0.05, +0.05]$, and $[-0.05, +0.05]$, respectively. After the fuzzification process, we can use the famous Mamdani inference mechanism to perform fuzzy reasoning.

3.2.2. Membership Functions

As membership functions have an important impact on the control performance, we must consider the influences of selecting an appropriate membership function. Specifically, the resolution of membership functions should be adjusted according to the errors (Wang et al., 2017). For example, we can choose low-resolution functions for bigger errors and high-resolution ones for the errors close to zero. In this work, the membership functions adopt Z-type, triangular, Gaussian and S-type, and the membership functions of the input and the output fuzzy sets for defuzzification are depicted in Fig. 8 and Fig. 9, respectively.

3.3. Linear Quadratic Regulator PID Controller

In the optimal control theory, the ideal performance can be obtained by calculating the control law based on the quadratic performance index. Here we integrate the quadratic performance index with the conventional PID controller, forming the LQR-PID controller, as shown in Fig. 10. In accordance with the conventional PID controller, $w(t)$ is the reference trajectory, $e(t)$ is the tracking error, and the $d(t)$ is the external disturbance. The major difference is that the LQR-PID takes the least sum of the absolute tracking error and the control increment as the performance index. The overall objective of the LQR-PID controller is to adaptively regulate the system so as to minimize its long-term average cost (Faradonbeh et al., 2020). The system can realize the weighted constrained control of the tracking error and the control increment by continuously changing the control
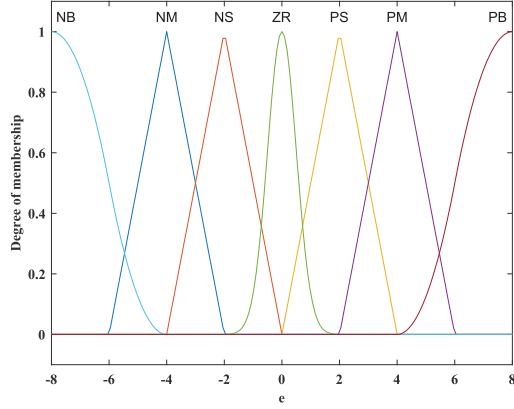
(a) Fuzzy sets of input variable e.
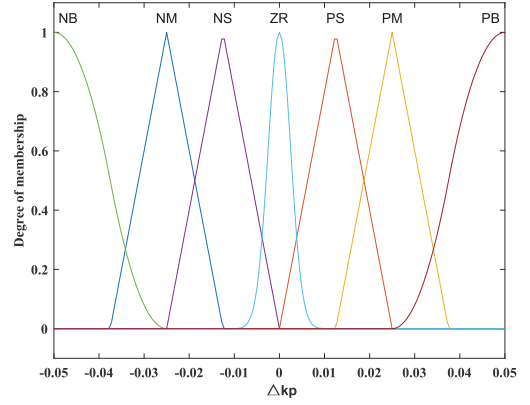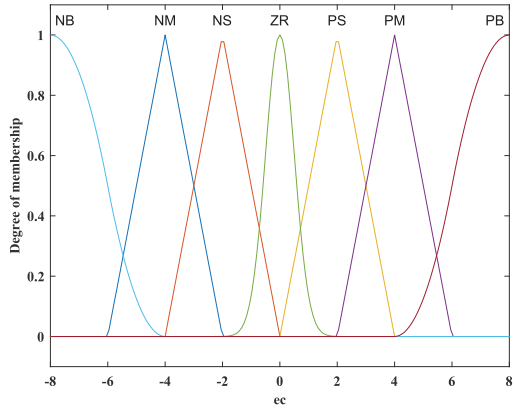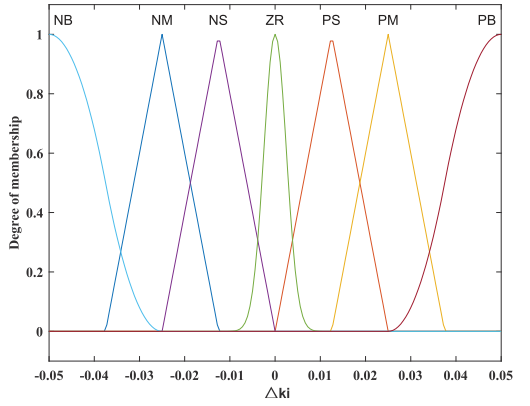
(b) Fuzzy sets of input variable ec.

Figure 8: Membership functions of the input fuzzy sets.

gains of the PID controller. Here we set a cost function as

$$E(k) = \frac{1}{2} \left(P \left(w(k) - y(k) \right)^2 + Q\Delta^2 u(k) \right), \qquad (23)$$

where P and Q are the weighted coefficients of the error and the control increment, respectively; $y(k)$ is the system output and $\Delta u(k)$ is the control increment. The control variable of the LQR-PID controller is expressed as

$$u(k) = u(k-1) + K \sum_{i=1}^{3} w_i'(k) x_i(k), \qquad (24)$$

where K is the proportional coefficient of the neuron. A bigger value of K can result in faster response, but it may also produce a large amount of overshoot and even cause system oscillations. In the case of an increase in the time delay of the controlled object, the value of K must be reduced to ensure the system stability. In the above equation, $w_i'(k)(i = 1, 2, 3)$ denotes the weighted coefficients of control gains of k_p, k_i

(a) Fuzzy sets of output variable Δk_p.

(b) Fuzzy sets of output variable Δk_i.
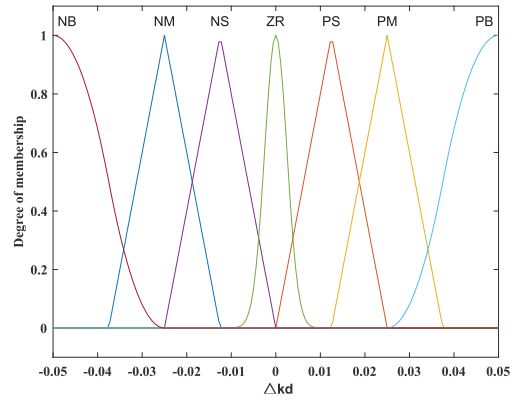
(c) Fuzzy sets of output variable Δk_d.

Figure 9: Membership functions of the output fuzzy sets.

and k_d, respectively, and they can be calculated as follows.

$$w_i'(k) = w_i(k) / \sum_{i=1}^{3} |w_i(k)| \quad (i = 1, 2, 3),$$

$$w_i(k) = w_i(k-1) + \eta_i K [Pb_0 e(k) x_i(k) - \qquad (25)$$

$$QK \sum_{i=1}^{3} \left(w_i(k) x_i(k) \right) x_i(k)],$$

The hyper-parameters used in the LQR-PID controller.

Item	P	Q	K	η_i	w_1	w_2	w_3	b_0
Value	0.01	1	0.01	0.25	0.8	5	0.8	0.02

Table 3
The initial parameters of three PID controllers.

Parameters	Type		
	PID	Fuzzy-PID	LQR-PID
$k_e, k_{ec}, k_p, k_i, k_d$		0.001,0.001,1.3,1,1.1	
Kp, Ki, Kd	0.5,0.1706,0.6479	0.78,0.1706.0.6479	0.78,0.1706,0.6479
Disturbance	0.1	0.1	0.1
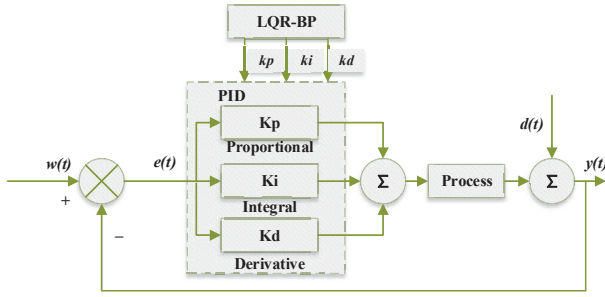
Figure 10: Illustration of the LQR-PID controller.

where $\eta_i (i = 1, 2, 3)$ is the learning rate of the control gains of k_p, k_i and k_d, respectively, b_0 is the initial value of the system output. As explained previously, $e(k)$ means the tracking error, so we use $x_1(k) = e(k)$, $x_2(k) = e(k) - e(k-1)$, and $x_3(k) = e(k) - 2e(k-1) + e(k-2)$ to denote the tracking error, the change of the error, and the change of the error rate, respectively. In this work, the hyper-parameters of the LQR-PID controller are listed in Table 2.

4. Experiment and Results

In this section, we evaluate the performance of the proposed MPC approach to the slurry pipeline transportation system. In order to demonstrate its advantages, we take the three PID controllers discussed in Section 3 as the baseline for comparison. We will first present the simulations results, and then discuss the experiment results obtained in a designed physical platform.

4.1. Evaluation in Simulations
4.1.1. Simulation Setup

To simulate the slurry pipeline transportation system, we use the process model established in Eq. 2. As depicted in Fig. 2, the relationship between the input frequency of the inverter and the control variable can be described by the proportion term, so we can obtain the transfer function

$$Gp = 5 \times Gp_1. \tag{26}$$

The parameters of the transfer function are fitted based on the following conditions. First, the sample time is set to 0.1s

and the continuous transfer function, discussed in Eq. (2), can be discretized. Then the differential evolution algorithm can be used to perform global optimization to fit the parameters (i.e., order, time delay, time constants of the inertia part) of the process model. The initial frequency of the converter is 5Hz, the cut-off frequency is 10Hz, the volume concentration of slurry is 20%, the diameter of slurry particles is $1.1mm$, the particle density is $2540kg/m^3$ and the slope change time is 30s. According to the final prediction errors in simulations, the error of the first-order model is 6.5×10^{-4}, the error of the second-order model is 4.12×10^{-4}, and the error of both the third-order and fourth-order model is 4.09×10^{-4}. Therefore, we can find that, in the same condition, the second-order, the third-order and the fourth-order models can produce almost the same prediction error. Since a higher model will increase the computation time, we can claim that the transfer function of the second-order time-delay system can be accurate enough to describe the dynamic response of the slurry pipeline transportation problem studied in this work. According to the above configuration, we can obtain the parameters of the transfer function as

$$Gp = \frac{0.9109}{(2.0559s + 1)(2.1685s + 1)}e^{-2.3s}, \tag{27}$$

where the open-loop gain k is 0.9109, the time constants of the inertia part Tp_1 and Tp_2 are 2.0559 and 2.1685, respectively, and the time delay τ is 2.3s.

In the simulations, the proposed MPC approach and the three PID controllers are evaluated in the step responses based on the transfer function as in Eq. 27. The desired flow rate of slurry is set to 1m/s, and the time horizon is set to 50s. The initial parameters of the three PID controllers are listed in Table 3. In our MPC approach, the parameters are determined as follows: the sampling frequency p is set to 60, the prediction horizon m and the control horizon n are set to 30 and 2, respectively, and the initial parameter of Y_0 in Eq. 10 is set to $[0, 0, \cdots, 0]$.

4.1.2. Step Response without Disturbances

The simulated results of the step response by applying the four controllers are shown in Fig. 11, which depicts the system output and input curves of the step response without disturbances. The detailed comparison results are listed

Table 4
Comparison of step response without disturbances.

Parameters		Type			
		PID	Fuzzy-PID	LQR-PID	MPC
Flow rate(m/s)	Maximum	1.084	1.009	1.000	1.078
	Mean	0.9687	0.9676	0.9477	0.9872
	Std	0.1643	0.154	0.1328	0.1102
Response time(s)		31.5	17.3	31.2	9.4

in Table 4, which reports the maximum, mean and standard deviation (std) of the flow rate, and the response time.
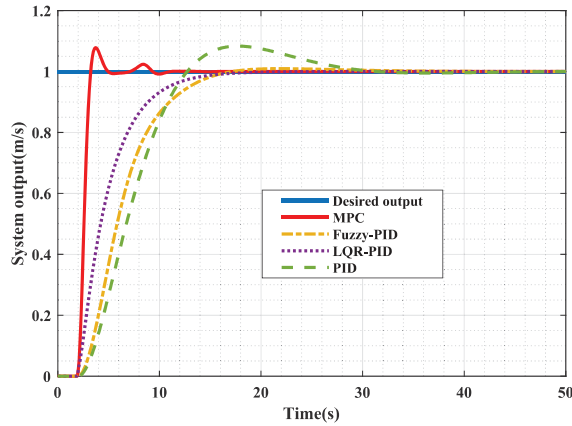
(a) The system output (the flow rate).
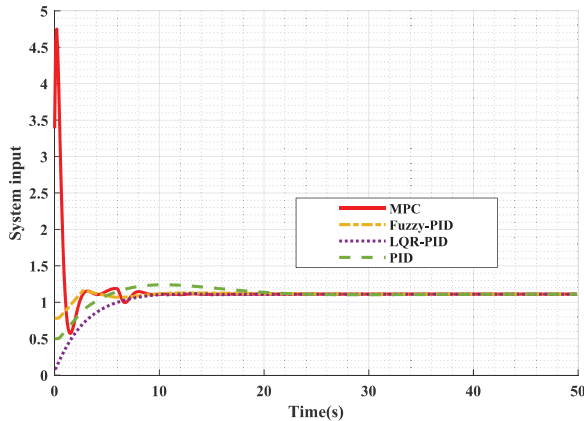
(b) The system input (the control variable u).

Figure 11: The step response in simulations without disturbances.

As shown in Fig. 11, the desired flow rate is set to 1m/s, which should be achieved by adapting control variable u. Thus, Fig. 11(b) depicts the system input curve, describing how the control variables of four controllers will be changed so that the system output can reach the desired flow rate. We can get a general impression that the control curves of the PID, Fuzzy-PID, and LQR-PID controllers are smoother but the responses are slower in comparison with the proposed MPC approach. As shown in Fig. 11(a), although the proposed MPC approach slightly fluctuates at the beginning, it

only spends 9.4s to reach to the desired flow rate with a little overshoot of 7.8%. The highest flow rate is 1.078m/s at 3.8s, and afterwards it can quickly converge to the desired stable value. Comparatively, the conventional PID controller shows the worst performance, which reaches highest flow rate of 1.084m/s at 17.7s, and takes 31.5s to realize the desired flow rate with an overshot of 8.4%. The Fuzyy-PID and LQR-PID controllers have almost no overshoot, but the required response time to the desired flow rate are 17.3s and 31.2s, respectively. With regard to the step response without disturbances, we can conclude that all of the controllers are able to achieve the goal, but the proposed MPC approach is the fastest one.

4.1.3. Step Response with Disturbances

In order to validate the ability of anti-interference of the proposed MPC approach, a disturbance of 0.1 amplitude is considered in the simulation. The system ouput and input curves of the step response are displayed in Fig. 12, and Table 5 also details the minimum flow rate and the response time when a disturbance is stimulated.

As can be seen in Fig. 12, the proposed MPC approach is superior to the other three PID controllers in terms of the anti-interference ability. When an external disturbance is suddenly loaded into the system, the proposed MPC approach only takes 3.3s to return back to the stable state (i.e., the desired flow rate). The LQR-PID controller takes the second place, spending 7.6s to achieve the goal state. Comparatively, to overcome the effects of the interference, the conventional PID controller and the Fuzzy-PID controller need 13.2s and 9.5s, respectively.

Based on the simulated results, we can conclude that the proposed MPC approach can outperform the conventional PID, Fuzzy-PID and LQR-PID controllers in chasing a desired flow rate of slurry. Since the above conclusions are only obtained based on the step response in simulation, we will verify whether the proposed approach still works in a physical platform.

4.2. Evaluation on a Physical Platform
4.2.1. Platform Design

As mentioned previously, in a CSD, the dredged materials need to be sucked up by a slurry pump and transported to the disposal area through a long-distance pipeline. When studying the slurry pipeline transportation system, we cannot use a real CSD to carry out the experiment due to the considerable cost and potential accidents. Thus, we design and build a special experiment platform, which models the

Table 5
Comparison of step response with a disturbance of 0.1.

Parameters	Type			
	PID	Fuzzy-PID	LQR-PID	MPC
Minimum flow rate(m/s)	0.9919	1.065	0.9940	0.9922
Response time(s)	13.2	9.5	7.6	3.3
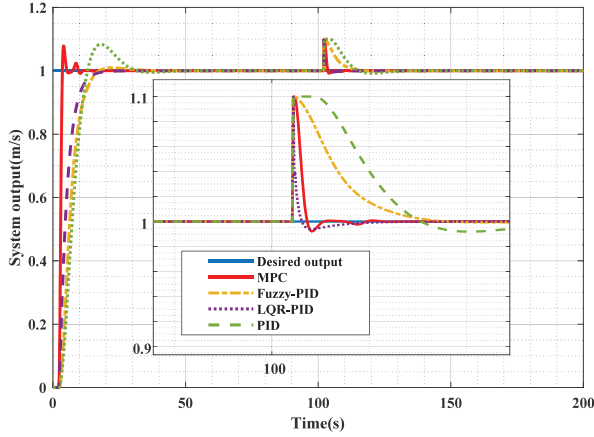
(a) The system output (the flow rate).
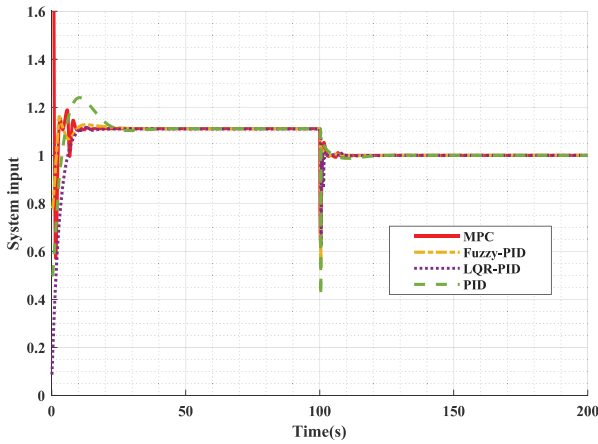
(b) The system input (the control variable u).

Figure 12: The step response in simulations with a disturbance of 0.1.

(a)

(b)

Figure 13: The designed experiment platform: (a) 3D illustration of the key components of the platform; (b) the physical platform used in our experiments.

slurry transportation process of a CSD, and, moreover, the slurry can circulate in the pipeline to improve the efficiency of the experiment, as shown in Fig. 13.

The main components of the platform include a 22kW slurry pump and its drive motor, a flowmeter, a densitometer, two pressure sensors, three valves, and a slurry hopper. The hopper is used to load coarse sand that can be gradually added to the circulated pipeline by opening the feeding valve. At the end of the experiment, the coarse sand can also be recycled into the hopper by opening the recycle valve. Similar to the simulations, in the experiment, the volume concentration of coarse sand is 20%, the diameter of particles is $1.1mm$, and the particle density is $2540kg/m^3$. Since the

slurry pipeline transportation problem is a dynamic process, many uncertainties can influence the control performance. For example, the concentration of slurry can be uneven, and the roughness of the pipeline can also affect the output of the control system. Although the experimental conditions are specific in this work, we still take account of disturbances to address uncertainties in the experiment. To this end, the interference valve of the physical platform is responsible for provoking disturbances by changing its opening degree.

The monitoring system of the physical platform consists of a host computer and a lower computer. All the controllers are realized in the host computer that generates control commands to be sent to the lower computer; whereas the lower computer is responsible for collecting the measurement data and directly controlling the inverter according to the control commands. The communication between the host and the lower computers is based on network flows and shared variables provided by LabVIEW. The experiment is divided into two groups, and we will first investigate the performance of four controllers without disturbances, in which the interference valve keeps open.

Table 6
Comparison of experiment results without disturbances.

Parameters		Type			
		PID	Fuzzy-PID	LQR-PID	MPC
0-1(m/s)	Maximum flow rate(m/s)	1.321	1.065	1.088	1.101
	Response time(s)	35	17	30	15
1-2(m/s)	Maximum flow rate(m/s)	2.042	2.032	2.026	2.053
	Response time(s)	21	21	19	7
2-3(m/s)	Maximum flow rate(m/s)	3.03	3.038	3.027	3.036
	Response time(s)	17	20	23	9

4.2.2. Experiment Results without Disturbances

We first perform the step response experiments in which the desired flow rate of slurry is set to 1m/s, 2m/s, and 3m/s, respectively. Thus, the four controllers are required to gradually chase those goals every 40s. Fig. 14 depicts the control performance, and Table 6 details the maximum flow rate and the response time in three step responses.
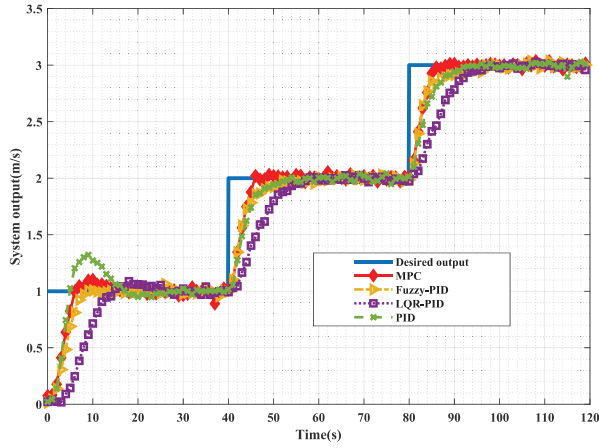
(a) The system output (the flow rate)
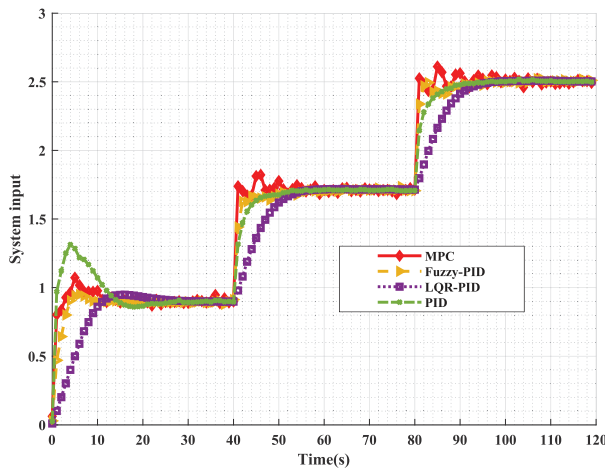
(b) The system input (the control variable u)

Figure 14: Performance comparison in the physical platform without disturbances.

Based on the experiment results, we can find that the system output curves show a corresponding correlation with the changes of the system input. In general, all of the four controllers are able to achieve the desired goals. To be more specific, during the first step response ($0 - 1$m/s), it can be seen that the proposed MPC approach arrives at the highest flow rate of 1.101m/s at 11s with a slight overshoot of 10.1%, and then reaches the desired flow rate at 15s. In contrast, the conventional PID controller is relatively quicker, but there is an overshoot of 32.1%, and finally it needs 35s to reach the desired flow rate. The Fuzzy-PID controller reaches the highest value of 1.065m/s at 6s with an overshoot of 6.5%, then achieves the desired flow rate at 17s, and gradually tends to the steady state. The responses of the LQR-PID controller are the slowest, and it spends 23s to reach the desired flow rate with an overshoot of 8.8%.

During the next step response ($1 - 2$m/s), the control curve of the proposed MPC approach can fluctuate to adapt itself so as to realize the desired state, spending only 7s to reach the desired flow rate with an overshoot of 5.3%. Comparatively, the other three PID controllers almost need triple time to realize the similar control effect. We can see that the PID controller spends 21s to reach the desired flow rate with an overshoot of 4.2%, and the Fuzzy-PID controller also takes 21s to reach the desired flow rate with an overshoot of 3.2%. The LQR-PID controller needs 19s to achieve the same state with an overshoot of 2.6%.

During the last step response ($2 - 3$m/s), the proposed MPC only takes 9s to reach the desired flow rate with an overshoot of 3.6%, whereas the response time of the other PID controllers needs twice as much time to achieve this goal. Specifically, the PID controller reaches the desired flow rate after 17s and then tends to the steady state with an overshoot of 3%, while the Fuzzy-PID controller reaches the desired flow rate after 20s and gradually comes to the steady state with an overshoot of 3.8%. The LQR-PID controller demonstrates the worst case that needs 23s to reaches the desired flow rate with an overshoot of 2.7%.

In brief, we can conclude that, in comparison with other controllers, the proposed MPC approach can produce the fastest response to maintain the desired flow rate. In this work, we do not particularly address how to maintain the critical flow rate, as it will be determined by many factors such as the particle diameter, pipeline diameter, and slurry concentration. Instead, we intent to show that whatever the desired flow rate is, the control systems is able to achieve this goal. Thus, the critical flow rate can be a special case

of the desired goals. In Fig. 14, we can also notice that the proposed MPC approach always can provide the best performance along with the increase of the desired flow rate.

4.2.3. Experiment Results with Disturbances

As mentioned previously, we can add disturbances to the circulated pipeline transportation system by changing the opening degree of the interference valve, as shown in Fig. 13. In the experiment, we set the desired flow rate to 2 m/s, and load the disturbances to the slurry pipeline transportation system by adjusting the opening degree of the interference valve from 100% to 50%, and the time spent for changing the interference valve is about 10s. Fig. 15 illustrates how the four controllers adapt the control variable, so as to cope with occasional disturbances, and Table 7 details the minimum/maximum flow rate, and the response time.
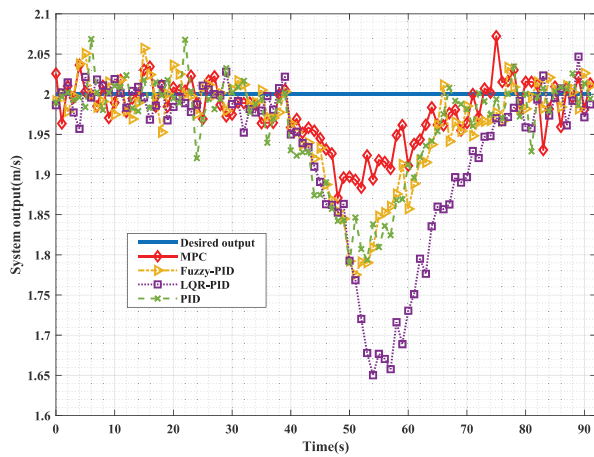
(a) The system output (the flow rate)
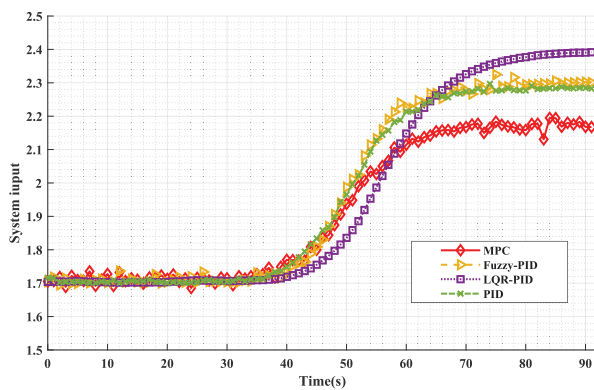
(b) The system input (the control variable u)

Figure 15: Performance comparison in the physical platform with disturbances.

As depicted in Fig. 13, the proposed MPC approach can demonstrate a superior ability of anti-interference in comparison with others PID controllers. When the opening degree of the interference valve is adjusted from 100% to 50% within 10s, the pipeline needs more power to maintain the desired flow rate. We can see that the control curve of the proposed MPC approach is relatively smooth than others,

and it takes 29.1s to return back to the steady state. Comparatively, the conventional PID and Fuzzy-PID controllers are moderately effective in resisting disturbances, and their response times are 30.4s and 30.6s, respectively. We can also explicitly identify that the LQR-PID controller is the worst case, and it costs 40.7s to return back to the desired flow rate. Moreover, the minimum flow rate of the LQR-PID controller even reaches to 1.65m/s, which may cause a potential risk of blockage. Thus, we can conclude that the proposed MPC approach outperforms the other PID controllers in controlling the flow rate of slurry, whenever the desired flow rate changes, or the disturbances are loaded into the pipeline transportation system.

5. Conclusions

The flow rate control of slurry (with coarse particles) in pipeline transportation is of great significance for saving energy and avoiding pipeline blockage for a CSD. However, most existing methods of controlling the flow rate in pipelines focus on transporting homogeneous materials, such as mineral slurry, oil or coal fly ash, and they are only proved by numeral simulations. In this work, we propose a MPC approach to address the slurry pipeline transportation problem for a CSD. To validate the effectiveness of the proposed approach, we have designed and built a physical experiment platform. To demonstrate the advantages of the proposed approach, we have also implemented three PID (i.e., conventional PID, Fuzzy-PID and LQR-PID) controllers for comparison. In the experiments, we first evaluated the step responses in simulations with and without disturbances, and then use the physical platform to examine the performance of reaching the desired flow rates with and without disturbances. The experiment results show that the proposed MPC approach can provide a competitive solution to the slurry pipeline transportation problem for a CSD.

References

Bai, S., Li, M., Kong, R., Han, S., Li, H., Qin, L., 2019. Data mining approach to construction productivity prediction for cutter suction dredgers. Automation in Construction 105, 102833.

Bobal, V., Kubalcik, M., Dostal, P., Matejicek, J., 2013. Adaptive predictive control of time-delay systems. Computers and Mathematics with Applications 66, 165–176.

Cutler, C.R., Ramaker, B.L., 1980. Dynamic matrix control-a computer control algorithm, in: Joint Automatic Control Conference, p. 72.

Faradonbeh, M.K.S., Tewari, A., Michailidis, G., 2020. On adaptive linear–quadratic regulators. Automatica 117, 108982.

Grüne, L., Pannek, J., 2017. Nonlinear model predictive control, in: Nonlinear Model Predictive Control. Springer, pp. 45–69.

Kouvaritakis, B., Cannon, M., 2016. Model predictive control : classical, robust and stochastic. Journal of Control ence and Engineering 2012, 5.

Long, R., Quan, S., Zhang, L., Chen, Q., Zeng, C., Ma, L., 2015. Current sharing in parallel fuel cell generation system based on model predictive control. International Journal of Hydrogen Energy 40, 11587–11594.

Moon, U.C., Lee, K.Y., 2009. Step-response model development for dynamic matrix control of a drum-type boiler–turbine system. IEEE Transactions on Energy Conversion 24, 423–430.

Morari, M., Lee, J.H., 1999. Model predictive control: past, present and future. Computers & Chemical Engineering 23, 667–682.

Table 7
Comparison of experiment results with disturbances.

Parameters		Type			
		PID	Fuzzy-PID	LQR-PID	MPC
Flow rate(m/s)	Minimum	1.79	1.775	1.65	1.871
	Maximum	2.069	2.057	2.047	2.072
Response time(s)		30.4	30.6	40.7	29.1

Priyanka, E., Maheswari, C., Meenakshipriya, B., 2016. Parameter monitoring and control during petrol transportation using plc based pid controller. Journal of applied research and technology 14, 125–131.

Priyanka, E., Maheswari, C., Thangavel, S., 2018. Online monitoring and control of flow rate in oil pipelines transportation system by using plc based fuzzy-pid controller. Flow Measurement and Instrumentation 62, 144–151.

Ramdani, A., Grouni, S., 2017. Dynamic matrix control and generalized predictive control, comparison study with imc-pid. International Journal of Hydrogen Energy 42, 17561–17570.

Razvarz, S., Vargas-Jarillo, C., Jafari, R., Gegov, A., 2019. Flow control of fluid in pipelines using pid controller. IEEE Access 7, 25673–25680.

Rullo, P., Degliuomini, L.N., Garcia, M., Basualdo, M., 2014. Model predictive control to ensure high quality hydrogen production for fuel cells. International journal of hydrogen energy 39, 8635–8649.

Singh, M.K., Kumar, S., Ratha, D., Kaur, H., 2017. Design of slurry transportation pipeline for the flow of muti-particulate coal ash suspension. International Journal of Hydrogen Energy 42, 19135–19138.

Sinha, S.L., Dewangan, S.K., Sharma, A., 2017. A review on particulate slurry erosive wear of industrial materials: In context with pipeline transportation of mineral- slurry. Particulate Science and Technology 35, 103–118.

Tang, J., Wang, Q., Zhong, T., 2009. Automatic monitoring and control of cutter suction dredger. Automation in construction 18, 194–203.

Ting, X., Xinzhuo, Z., Miedema, S.A., Xiuhan, C., 2019. Study of the characteristics of the flow regimes and dynamics of coarse particles in pipeline transportation. Powder Technology 347, 148–158.

Vazquez, S., Rodriguez, J., Rivera, M., Franquelo, L.G., Norambuena, M., 2016. Model predictive control for power converters and drives: Advances and trends. IEEE Transactions on Industrial Electronics 64, 935–947.

Wang, B., Fan, S., Jiang, P., Xing, T., Fang, Z., Wen, Q., 2020. Research on predicting the productivity of cutter suction dredgers based on data mining with model stacked generalization. Ocean Engineering 217, 108001.

Wang, T., Gao, H., Qiu, J., 2015. A combined adaptive neural network and nonlinear model predictive control for multirate networked industrial process control. IEEE Transactions on Neural Networks and Learning Systems 27, 416–425.

Wang, Y., Jin, Q., Zhang, R., 2017. Improved fuzzy pid controller design using predictive functional control structure. ISA transactions 71, 354–363.

Wei, C., Ni, F., Chen, X., 2019. Obtaining human experience for intelligent dredger control: A reinforcement learning approach. Applied Sciences 9, 1769.